

RESEARCH

Open Access



Quantitative stable isotope probing (qSIP) and cross-domain networks reveal bacterial-fungal interactions in the hyphosphere

Giovana S. Slanzon^{1*}, Mengting Yuan^{1,2}, Katerina Estera-Molina^{2,3}, Aaron Chew³, Steve J. Blazewicz³, Michael Allen³, Mary K. Firestone², Jennifer Pett-Ridge^{2,3} and Nhu H. Nguyen^{1*}

Abstract

Background Interactions between fungi and bacteria have the potential to substantially influence soil carbon dynamics in soil, but we have yet to fully identify these interactions and partners in their natural environment. In this study, we stacked two powerful methods, ¹³C quantitative stable isotope probing (qSIP) and cross-domain co-occurrence network, to identify interacting fungi and bacteria in a California grassland soil. We used in-field whole plant ¹³CO₂ labeling along with sand-filled ingrowth bags (that trap fungi and hyphae-associated bacteria) to amplify the signal of fungal-bacterial interactions, separate from the bulk soil background.

Results We found a total of 54 bacterial ASVs and 9 fungal OTUs that were significantly ¹³C-enriched. These were saprotrophic and biotrophic fungi, and motile, sometimes predatory bacteria. Among these, 70% of all ¹³C-enriched bacteria identified were motile. Notably, we detected fungal-bacterial network links between a fungal OTU of the genus *Alternaria* and several bacterial ASVs of the genera *Bacteriovorax*, *Mucilaginibacter*, and *Flavobacterium*, providing empirical evidence of their direct interactions through C exchange. We observed a strong positive co-occurrence pattern between predatory bacteria of the phylum Bdellovibrionota and fungal OTUs, suggesting the transfer of C across the soil food web.

Conclusions To date, our ability to associate microbial co-occurrence network patterns with biological interactions is limited, but the incorporation of qSIP allowed us to more precisely detect interacting partners by narrowing in on the taxa that were actively incorporating plant-fixed, fungal-transported labeled substrates. Together, these approaches can help build a mechanistic understanding of the complex nature of fungal-bacterial interactions in soil.

Introduction

In soil, fungi and bacteria share the same physical space and assemble into dynamic communities that consume, process and translocate plant-derived organic matter that contribute to nutrient cycling [1]. In this space, the “hyphosphere” (i.e., the area of fungal influence surrounding hyphae) impacts the assembly and activity of bacterial communities [2], and potentially leads to a selection of a core microbiome [3, 4]. Functionally, these two groups of organisms complement each other and occupy distinct physical soil habitats [5], where fungi are better at metabolizing complex organic substrates and

*Correspondence:

Giovana S. Slanzon
giovanas@hawaii.edu

Nhu H. Nguyen
nhu.nguyen@hawaii.edu

¹ University of Hawai'i at Mānoa, Honolulu, USA

² University of California Berkeley, Berkeley, USA

³ Lawrence Livermore National Laboratory, Livermore, USA



© The Author(s) 2025. **Open Access** This article is licensed under a Creative Commons Attribution-NonCommercial-NoDerivatives 4.0 International License, which permits any non-commercial use, sharing, distribution and reproduction in any medium or format, as long as you give appropriate credit to the original author(s) and the source, provide a link to the Creative Commons licence, and indicate if you modified the licensed material. You do not have permission under this licence to share adapted material derived from this article or parts of it. The images or other third party material in this article are included in the article's Creative Commons licence, unless indicated otherwise in a credit line to the material. If material is not included in the article's Creative Commons licence and your intended use is not permitted by statutory regulation or exceeds the permitted use, you will need to obtain permission directly from the copyright holder. To view a copy of this licence, visit <http://creativecommons.org/licenses/by-nc-nd/4.0/>.

bacteria are more efficient in using simpler organic compounds [6, 7]. Given that fungi and bacteria have some overlap in spatial niches and nutrient resources, the interactions between them, whether competitive or synergistic, are expected to have a substantial impact on global soil nutrient cycling [8]. However, despite the ubiquity of their distribution across all soil ecosystems, deciphering the dynamic and complex interactions within the hyphosphere and linking them to soil processes still remains a challenge. This is especially true for quantitative assessments of these interactions. By having a more quantitative understanding of fungal-bacterial interactions in the soil, especially in relation to a specific nutrient, we could better characterize how these microorganisms contribute to nutrient cycling, organic matter decomposition, and their role in the soil food web.

As a first step to understanding fungal-bacterial interactions and their functional contributions to soil processes, some studies have used quantitative stable isotope probing (qSIP) [9] to track the fate of C fixed by plants, transferred to fungi such as arbuscular mycorrhizal fungi (AMF), and eventually to hyphosphere bacteria [10, 11]. This transfer can occur through the assimilation of fungal-released compounds by bacteria associated with the hyphae [12] or by bacteria predating directly on the hyphae [13]. Some of the carbon from microbial necromass may come to persist as part of mineral associated organic matter [11, 14]. The use of qSIP in these studies established the connection between microbial identity and their functional activity in their natural environment. More specifically, these studies showed cross-domain interactions among arbuscular mycorrhizal fungi (AMF), ammonia-oxidizing archaea, and many types of bacteria [10, 11]. qSIP has also been used to provide quantitative measurements of potential antagonistic relationships between predatory and non-predatory bacteria; a recent qSIP meta-analysis suggests predatory bacteria grew 36% times faster and assimilated C at a 211% higher rate than non-predatory bacteria [15]. While these studies showed the pathways of C flow through the soil, the characterization of soil bacteria actively consuming fungal C through interactions with fungal hyphae in situ remains to be identified.

Recent developments in network analysis techniques have offered more comprehensive characterization of community composition and abundance. Co-occurrence patterns identified through networks have increased our capacity to identify potential interactions among community members. While network analyses of individual groups of organisms are frequently used to infer interactions, a small number of studies have explored cross-domain co-occurrence networks of both bacteria and fungi. These studies show broad

connections between network topology and the links among network members. For example, fungal-bacterial co-occurrence patterns can differ between arbuscular mycorrhizal fungi and nonmycorrhizal fungi across soil niches [16], they may be affected by different forms of organic nutrients [17], and may be connected to soil aggregate structure [18]. The network links among fungi and bacteria within a substrate suggest potential indicators of bacteria consumption of fungal biomass [16]. This has been experimentally observed by identifying isotopically labeled bacteria and fungi that fed on ^{13}C and ^{15}N labeled fungal necromass as a substrate [19]. However, a key limitation of ecological network analysis is its reliance on pairwise correlations, which may not accurately represent the biological interactions in natural environments. Moreover, this approach typically provides only a static snapshot at a single time point, neglecting the dynamic nature of ecosystems as well as potentially capturing links between taxa that are inactive during that time. By focusing solely on relative abundance patterns between pairs, we miss the broader community context, overlooking other organisms that likely influence these relationships. Additionally, spatial variation and ecological niche differences, particularly between fungi and bacteria [20], are often not adequately considered, which may lead to an incomplete understanding of ecosystem complexity when constructing a network. Despite their limitations, cross-domain networks provide ways to condense the high-dimensionality of microbiome data and are increasingly used to hypothesize the nature of fungal-bacterial interactions.

While qSIP alone can be used to measure growth rates or indicate which fungi and bacteria are part of the plant-derived soil C cycle, when combined with co-occurrence network analysis, can more precisely hypothesize the abundance patterns between the microorganisms that exist in an environment in relation to their nutrient dynamics. We propose that combining these two complementary methods (^{13}C qSIP with isotope-enabled cross-domain network analysis), will allow us to better target interacting fungal-bacterial partners and generate more directed hypotheses. Here we demonstrate the utility of this approach in a grassland soil system. We followed the path of ^{13}C labeled isotopes fixed by plants into the hyphosphere and found strong links among the active bacteria and fungi involved in C cycling that are more precisely identified compared to total microbial community networks calculated from unlabeled data. Together, these approaches can significantly contribute towards building a mechanistic understanding of the complex nature of fungal-bacterial interactions in soil.

Material and methods

Site characteristics, sample collection, and labeling

This study was conducted in March 2020 in a California annual grassland at the University of California Hopland Research and Extension Center (Hopland, CA, 39.004011–123.086001, 260 m asl), on traditional, ancestral, and unceded lands of the Shóqowa and Hopland people. The grassland is dominated by naturalized annual Mediterranean grasses and forbs, particularly *Avena barbata* (slender wild oat), on an Ashokawna-Witherell complex soil. The soil at the field site belongs to the Squawrock-Witherell complex, a loamy-skeletal, mixed, superactive, thermic Typic Haploxeralf. The underlying parent material is colluvium derived from sandstone. Detailed site characteristics and soil physico-chemical properties has been reported in Fossum et al. [14]. We used six ingrowth bags made of 50 μm nylon mesh, filled with 70 g of quartz sand that had been acid washed to remove adhering organic matter, baked at 150 °C, and neutralized to a pH of 7. Bags were cleaned in 70% ethanol prior to use. This mesh size allows fungi but not roots to grow through, thus acting as a trap for fungi and the bacteria associated with fungal hyphae. Unlike rhizosphere soils, hyphosphere soil is often difficult to physically separate and sample; this trap method (ingrowth bags) creates an environment that isolates fungal-bacterial interactions away from the soil background, while still maintaining edaphic conditions of the in situ environment. As expected, the bacterial and fungal communities observed in the sandbags were a subset of the communities found in the bulk soil (Supplemental Fig. S1). We reasoned that since the sand is a nutrient-poor substrate, and that fungal hyphae transport nutrients into these sandbags, the bacteria found there would more likely be interacting directly with the fungi.

Samples collected for this study are a subset from a larger ^{13}C labeling field experiment. Field site, plot establishment, and ^{13}C labeling illustration has been previously shown in Fossum et al. [14]. Each of the six ingrowth bags was inserted into the soil 15 cm deep by a simple slit to minimize disturbance, each within a 40-cm diameter collars that were within 180 \times 130 cm plots that had been seeded with *A. barbata* for the purpose of this experiment to ensure it was the dominant grass species. The collars were designated to be fitted with an above-ground cylindrical chamber for labelling plants with either ^{12}C or ^{13}C -CO₂. The bags were incubated in situ for 12 days prior to start of a ^{13}C plant labeling study, to allow hyphae and associated bacteria to enter and colonize the sand matrix. A total of six chamber were used in this study. During a period of exponential plant growth in the spring, when both soil moisture and sunlight are optimized in this Mediterranean climate, three of the

collars became bases for ^{13}C labeling chambers and were labeled with ^{13}C for 8 continuous days, and the other three collars became bases for ^{12}C chambers that were exposed to ^{12}C as a control for the same amount of time. For the labeling study, ^{12}C and 99 atom% ^{13}C (Sigma-Aldrich) were delivered to their respective labeling chambers (measuring 0.41 m in diameter and 0.9 m in height, enclosing the entire collar) in plots using an automated CO₂ delivery system [14]. Briefly, CO₂ analyzers (a Picarro G2201-i and SBA-5 IRGA) monitored the headspace CO₂ for ^{13}C and ^{12}C chambers respectively. The results were used to calculate the amount of gas to be added to each chamber based on current CO₂ headspace concentration and photosynthetically active radiation (PAR). Ingrowth bags were harvested the day after ^{13}C labeling ceased. The sand from the ingrowth bags was carefully extracted and stored at –80 °C prior to DNA extraction. The experiment had an $n=3$ for each isotope treatment.

DNA extraction, fractionation, and quantification

Due to low biomass within the sand, all 105 g of sand from each ingrowth bag was used for DNA extraction using a standard CTAB buffer-chloroform phase extraction. The extracted DNA was quantified using a NanoDrop One spectrophotometer (ThermoFisher Scientific, USA) to assess purity and Qubit 3.0 fluorometer (ThermoFisher Scientific, USA) to assess concentration. For each replicate (a single physical sample) 1 μg of DNA was subjected to ultracentrifugation in a cesium chloride density gradient, then separated into 22 fractions [10]. Fractions with low concentration of DNA at the beginning (fractions 1 and 2) and end of the gradient (fractions 18–22) were not included in the following steps. To have enough DNA to prepare the libraries and conduct quantitative polymerase chain reaction (qPCR) analysis targeting both bacteria and fungi, all other fractions were combined into 7 fraction groups based on their density (1.7473–1.7491 g/ml, 1.7186–1.7220 g/ml, 1.7119–1.7165 g/ml, 1.7065–1.7096 g/ml, 1.6993–1.7050 g/ml, 1.6949–1.6985 g/ml, 1.6613–1.6847 g/ml). The combination of fractions into groups was based on the minimum amount of DNA needed to conduct the set of analysis proposed in this study (amplicon sequencing and qPCR for bacterial and fungal communities), which totals a minimum of 20 ng of DNA per fraction group. The final density of each combined fraction group was calculated proportionally by averaging the density values of the fractions that were combined.

Amplicon libraries were prepared for each of the 7 fractions groups of all 6 biological samples with a two-step PCR process by amplifying the V4 region of the bacterial and archaeal 16S rRNA gene using the primers 515F

[21] and 806R [22], and the ITS2 region of the fungal ITS rRNA gene using the primers ITS5.8S-fun and ITS4-fun [23]. Polymerase chain reaction (PCR) analysis was conducted using the NEBNext Ultra II Q5 Master Mix (New England Biolabs, USA), containing a high-fidelity polymerase (Bio-Rad Laboratories, USA). The final library was sequenced on a single Illumina MiSeq 300PE run. PCR negative controls and a mock community as positive controls were added along with the experimental samples [24].

Sequences were processed using QIIME2 v2022.2 and available plugins [25]. Raw sequences were demultiplexed, paired and denoised using DADA2 [26] into amplicon sequence variants (ASVs). ITS sequences were further clustered at 97% similarity using the VSEARCH plugin [27] into 97% operational taxonomic units (OTUs). This clustering step was necessary to reflect expected OTUs found in our fungal mock community [24]. Representative sequences were identified using the sklearn classifier in QIIME2, trained on the SILVA v138 [28] database for 16S and VSEARCH classifier in QIIME2, trained on the UNITE v8.3 database [29] for ITS. Mitochondria, chloroplast, and unassigned sequences in the 16S dataset, and non-fungal sequence from the ITS dataset were removed. Fungal OTUs were further identified using BLAST against the type specimen database. Due to the heterogeneity of the fungal ITS gene, clustering (typically at 97%) is necessary to reduce inflation of richness and better reflect the species level status of these organisms [24]. Overall, our goal was to bring these two different datasets with different marker genes closer to the operational species level prior to further analysis. Trophic guild information was identified using the FUNGuild v2 database [30]. Motile bacteria were identified through literature search.

Additionally, amplicon libraries targeting the bacterial and archaeal 16S rRNA gene and fungal ITS gene were prepared for each of the six physical sandbag samples (prior to fractionation for qSIP analysis) and for six bulk soil samples collected from corresponding plots, using the same methods as the qSIP dataset.

Quantitative PCR

We determined the total numbers of bacterial 16S rRNA gene copies in each density fraction by qPCR using the primers Eub 338/518 [31] to target bacteria, and the primers ITS86F/ITS4 [32] to target fungi. These primers were chosen because internal testing showed that they had the best efficiency in qPCR reactions. For qPCR analysis, samples were analyzed in triplicate with 15 μ L reactions containing 5 μ L of template DNA (normalized to 0.125 ng/ μ L), 7.5 μ L Power Up SYBR Master Mix (Applied Biosystems), 1 μ L nuclease-free water, and 1.5 μ L primers

(10 μ M). Quantification of bacterial and fungal genes was determined using a standard curve. A single synthetic DNA molecule containing the 16S sequence from *Escherichia coli* and the ITS sequence from *Aspergillus sydowii* was created in silico as the standard for bacterial and fungal quantification. The gBlock standard was diluted to a working concentration of 1×10^8 copies/ μ L and stored at -80 °C. At the time of the qPCR assay, seven-point standard curves were prepared using tenfold dilutions of the gBlock stock from 1×10^1 to 1×10^7 copies/ μ L and nuclease-free water as the negative control. PCR cycling conditions included initial incubation at 50 °C for 2 min, initial denaturation at 95 °C for 2 min, followed by 40 cycles of 95 °C for 15 s and 60 °C for 60 s for both bacteria and fungi. SYBR green fluorescence was collected at the end of each extension cycle along with a final melt curve analysis. Data was collected using QuantStudio 3 (Applied Biosystems) and data was analyzed using the Design & Analysis Software v2.6.2 (Applied Biosystems). PCR efficiencies determined from the standard curves ranged from 99 to 100% and slope -3.32 for bacteria, and 98–100% and slope -3.35 for fungi, with all standard curves having $R^2 > 0.99$.

Quantitative stable isotope probing

The qSIP method quantifies the change in DNA density of each taxon caused by isotope incorporation relative to the baseline densities of the DNA of individual taxa without exposure to isotope tracers. Isotope incorporation was quantified for bacteria and fungi by converting taxon-specific shifts in DNA density to ^{13}C excess atom fraction (EAF) according to the equations detailed in [9, 33] using the qSIP2 R package [34]. While these equations were originally optimized for bacteria and archaea, they have also been used to estimate ^{13}C EAF for fungi [10, 35]. The EAF value reflects the proportion of labeled carbon atoms that are assimilated into the genomic DNA of organisms that are actively growing and synthesizing new DNA. For example, an EAF value of 0.2 indicates that 20% of the carbon atoms within the gene targeted (16S or ITS) are ^{13}C labeled. For bacteria, qSIP analysis was limited to taxa that occurred in all 3 replicates and in at least 3 fractions of each replicate. For fungi, qSIP analysis was limited to taxa that occurred in all 3 replicates and in at least 1 fraction of each replicate. These parameters were chosen for each group to best represent the microbial diversity within the limited number of sample replications in this study. Bootstrap resampling with 1,000 iterations was used to calculate the 90% confidence intervals (CI) from the distribution of EAF estimates. We considered any ASV or OTU where the 90% lower confidence interval was greater than 0% ^{13}C EAF as significantly enriched.

Co-occurrence network analysis

We built a cross-domain network of ^{13}C -assimilating bacteria and fungi (enriched community network) as a novel way to identify potentially interacting partners through C exchange. The same methods were used to construct a total community (^{12}C) network. The networks were constructed using the molecular ecological network analyses (MENA) pipeline based on random matrix theory (RMT) [36]. For the enriched community (^{13}C) network, the first step was to select for taxa that significantly incorporated the heavy isotope based on qSIP analysis. All 63 labeled taxa (9 fungal OTUs and 54 bacterial ASVs) with lower 90% CI greater than 0% ^{13}C EAF were considered when constructing the network (Supplementary Table S1). For the construction of the total community (^{12}C) network, all 5259 taxa present in the unlabeled samples were considered, including 266 fungal OTUs and 4993 bacterial and archaeal ASVs. To ensure the reliability of correlation calculation, only ASVs and OTUs that were present in at least 11 of the 21 combined fractions from each of the labeled or unlabeled samples were included for correlation calculation [16, 36]. After this filtering step, a total of 58 taxa were kept for the construction of the enriched community (^{13}C) network and 454 for the construction of the total community (^{12}C) network. The distribution of the ASV/OTUs across all samples and fractions can be found in Supplemental Fig. S2. To allow comparisons between the two compositional datasets, a centered-log ratio (clr) transformation was performed for bacterial and fungal absolute abundance tables separately [37, 38] using the R package *microbiome* [39]. Next, the fungal and bacterial transformed datasets were combined and Spearman correlation coefficients were calculated between all pairs. A cut-off correlation threshold was selected automatically by the RMT approach to calculate the adjacency matrix. Network modularity was calculated using the greedy modularity optimization method [36]. Random networks were generated and topological parameters were calculated for both ecological and random networks [36]. The differences of topological parameters between ecological and random networks were evaluated using z-test [36]. The RMT cut-off for the total community network was 0.89 and for the enriched community network was 0.32. The different cut-offs allow us to adequately capture co-occurrence patterns according to each dataset. Networks were visualized using Gephi [40]. To identify the relationship between the fungal-bacterial links that appeared in the enriched community network, a linear model using the clr transformed abundance data of statistically significant pairs was fitted using the R package *ggpmisc* [41]. To compare the topological variation between the total community (^{12}C) and the enriched community (^{13}C) networks due to differences in

number of taxa from each dataset, a subset of the ASVs/OTUs from unlabeled samples was randomly selected to construct a mock network simulating the same number of taxa kept to construct the enriched community (^{13}C) network (9 fungal OTUs and 54 bacterial ASVs).

Results

We established a $^{13}\text{CO}_2$ labeling experiment in a sand-filled ingrowth bags system, where we inferred that ^{13}C from a pulse label was released by plant roots, consumed by rhizosphere fungi that extend beyond the rhizosphere into the ingrowth bags, and into the hyphosphere where the labeled substrate was assimilated by associated bacteria. After 8 days of $^{13}\text{CO}_2$ plant labelling, we observed evidence of ^{13}C -enrichment in microorganisms in our ingrowth bags, shown by an increase in DNA density between 12 and ^{13}C samples (Supplemental Fig. S3). The density gradient of fractionated samples ranged from 1.66 to 1.75 g/ml. The number of gene copies (determined by qPCR) ranged from 1.12 to 57.03 gene copies/ μl for bacteria/archaea and from 1.09 to 716.61 gene copies/ μl for fungi. Although relatively small, this observable shift was comparable to previous studies [10] and enough to detect significant incorporation of ^{13}C into individual taxa.

Many microorganisms in the ^{13}C ingrowth bags were isotopically enriched. Of the 7785 ASVs observed in the overall sequence dataset, 29 were archaeal and 7756 were bacterial. From these, 5470 ASVs were present in ^{13}C samples and 4993 were present in the ^{12}C samples. For fungi, we observed a total of 423 OTUs, with 305 in the ^{13}C samples and 266 in the ^{12}C samples. After applying qSIP criteria (detected in enough replicates and fractions, Supplementary Table S1), we identified 214 ^{13}C -enriched bacterial ASVs and 37 fungal OTUs. From this group, we further applied our significant enrichment criterion (lower 90% CI greater than 0% ^{13}C EAF), yielding a subset of 54 bacterial ASVs and 9 fungal OTUs that were significantly ^{13}C -enriched. We use this terminology because we have high confidence that these ASVs/OTUs represented microorganisms that have incorporated ^{13}C . ^{13}C enrichment varied widely for organisms within the major phyla of fungi and bacteria (Fig. 1). The fungal phyla Ascomycota and Basidiomycota were the most ^{13}C -enriched, with higher proportions of significantly labeled OTUs compared with other phyla. The bacterial phyla Actinobacteriota, Bacteriodota, Bdellovibrionota, Proteobacteria, and Verrucromicrobiota were some of the most ^{13}C -enriched; Bacteriodota and Proteobacteria had the highest number of significantly ^{13}C -enriched ASVs. We observed only a single ASV each of the Acidobacteria and Fibrobacterota, and two ASVs of the Cyanobacteria phyla, and no ^{13}C -enriched archaeal ASVs.

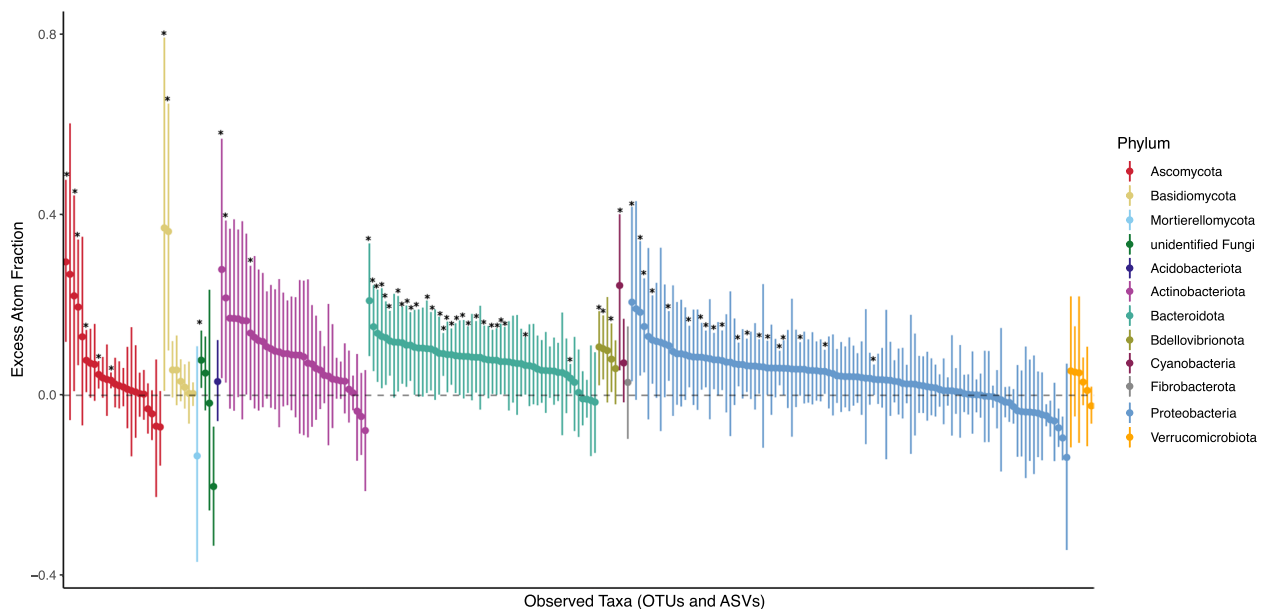


Fig. 1 Phyla of fungi and bacteria that were ^{13}C -enriched in sand-filled ingrowth bags after a $^{13}\text{CO}_2$ plant labelling experiment in a grassland soil. Each dot marks a single fungal OTU or bacterial ASV and represents the average excess atom fraction (EAF) with a 90% confidence interval. Bootstrap resampling was used to calculate the 90% confidence intervals (vertical bars) from the distribution of EAF estimates. Note that the OTU/ASVs shown include both significantly enriched and those with an enrichment confidence interval overlapping 0. * Indicates significantly enriched OTU/ASVs

Of the 37 ^{13}C -enriched fungal OTUs, 26 were assigned to functional groups using the FUNGuild database. Among the most highly ^{13}C -enriched taxa were saprotrophic or biotrophic fungi (plant pathogen or animal parasite) and motile bacteria (Fig. 2, Supplementary Table S2). These included the fungal genera *Coprinus* (saprotrophic), *Aspergillus* (saprotrophic), *Ijuhya* (animal parasite), and *Aureobasidium* (plant pathogen). At the individual OTU level, some of the most highly ^{13}C -enriched taxa were an OTU of the genus *Vishniacozyma* (saprotrophic), an OTU of the genus *Coprinus* (saprotrophic), and an OTU of the genus *Aspergillus* (saprotrophic). For bacteria the genera *Serinibacter*, *Calothrix*, *Ferribacterium*, and *Rhizobacter* had the highest ^{13}C -enrichment. At the ASVs level, among the highest ^{13}C -enriched ASVs were an ASV of the genus *Serinibacter*, an ASV of the genus *Calothrix*, and an ASV of the genus *Nocardioides*. Notably, 70% of ^{13}C -enriched bacterial ASVs (151 out of 214 bacterial ASVs) were motile.

We used network analysis on both unfractionated (total) microbial community and the ^{13}C enriched community data to identify potential fungal-bacterial interactions related to C dynamics. We compared a total community (^{12}C) with an enriched community (^{13}C) network to assess whether the same links can be found (Fig. 3). We observed 233 nodes and 589 total links in the total community (^{12}C) network, of which only 4 were fungal-bacterial

links. In contrast, 56 nodes and 914 links were observed in the enriched community (^{13}C) network, 137 of which were fungal-bacterial links. The topological properties of both networks were distinct, especially in relation to the number of edges per node (average degree). In addition, randomly generated networks differed from their corresponding ecological networks (Supplemental Table S3), indicating that the constructed cross-domain networks were non-random. Most notably, we found that compared to the total community (^{12}C) network, the enriched community (^{13}C) network had a much higher complexity, with fewer nodes and more edges (average degree of 32.64 in the ^{13}C network vs 5.05 in the ^{12}C network), and more fungal-bacterial links (15% in ^{13}C network vs 0.7% in ^{12}C network). Only one fungal-bacterial link was shared with the total community (^{12}C) network. In the enriched community (^{13}C) network, 6 of the 9 significantly ^{13}C -labeled fungal OTUs linked with bacteria, and 46 of the 54 significantly ^{13}C -labeled bacterial ASVs linked with fungi. Moreover, we constructed a mock network by randomly selecting the same number of taxa used to construct the enriched community network from the unlabeled dataset (Supplemental Table S3). This comparison showed that both the enriched community as well as the mock network had very similar overall topology, with greater number of fungal-bacterial links (137 in the ^{13}C network and 155 in the ^{12}C mock network), and lower RMT

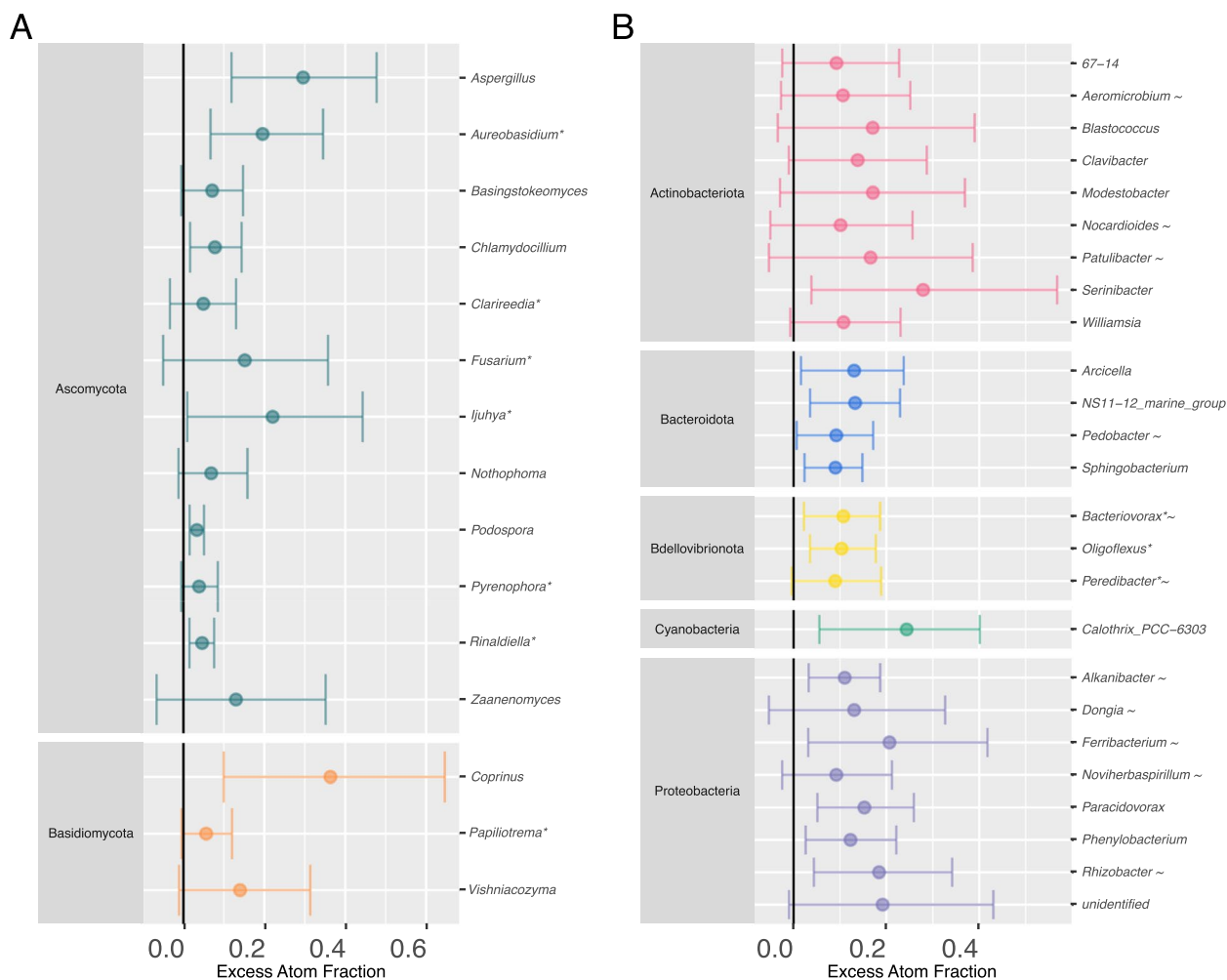


Fig. 2 Fungal (A) and bacterial (B) genera that were ¹³C-enriched in sand-filled ingrowth bags after a ¹³CO₂ plant labelling experiment in a grassland soil. Each dot represents the mean excess atom fraction (EAF) of all labeled bacterial ASVs and fungal OTUs, flanked by 90% confidence intervals of ¹³C EAF for the entire genus. The genera are grouped and colored by phylum. * indicates biotrophic organisms (animal parasitic or plant-pathogenic fungi; predatory bacteria). ~ indicates motile bacterial genera

cut-offs (0.32 for the ¹³C network and 0.31 for the ¹²C mock network) when compared with the total microbial community (¹²C) network. This suggests that the pattern observed in the enriched community (¹³C) network may be an attribute of the lower RMT cut-off or the reduced number of features used to construct the network.

We more thoroughly examined both the total community (¹²C) and enriched community (¹³C) networks to identify individual fungal-bacterial links with strong relationship ($R^2 \geq 0.65$) (Fig. 4). Of note in enriched community (¹³C) network were the strong positive fungal-bacterial links between the fungus *Alternaria* OTU3 and bacteria *Bacteriovorax* ASV2, *Mucilaginibacter* ASV3, and *Flavobacterium* ASV6. The fungus *Podospora* OTU1 strongly linked with the bacteria *Peredibacter* ASV1,

Oligoflexus ASV4, and *Pedobacter* ASV5 and ASV7. Strong positive links were also observed between the fungus *Aureobasidium* OTU2, *Ijuhya* OTU4 with *Bacteriovorax* ASV2. Fungal-bacterial links in the total community (¹²C) network are slightly different, where a fungal OTU of the genus *Chaetomium* linked with a bacterial ASV of the genus *Massilia*. The fungus *Podospora* OTU1 formed a strong link with an ASV of the genus *Chryseobacterium*. A fungal OTU of the genus *Cladorrhinum* linked with a bacterial ASV of the genera *Acinetobacter*, and a fungal OTU of the genus *Gibellulopsis* linked with a bacterial ASV of the genus *Duganella* (Supplemental Table S4). The link between the fungus *Podospora* OTU1 and the bacterial ASV of the genus *Chryseobacterium* was observed in both the total community (¹²C) and the

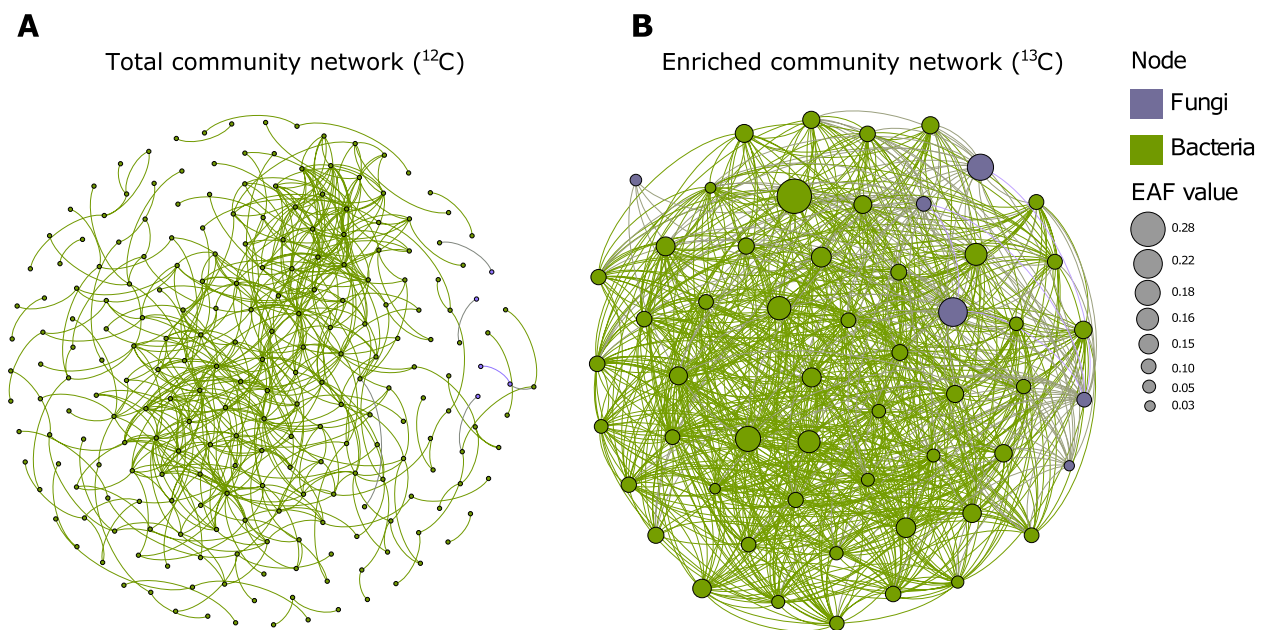


Fig. 3 Cross-domain co-occurrence networks were calculated across all fractions for total microbial (^{12}C) community (**A**) and enriched community after a $^{13}\text{CO}_2$ plant labelling experiment in sand-filled ingrowth bags in a grassland soil (**B**). Nodes are colored by domain (bacteria or fungi) and relative size within each network represents the degree of each node indicating the number of connections it has to other nodes. The node size in the enriched community (^{13}C) network represents the excess atom fraction (EAF) of each bacterial ASV or fungal OTU

enriched community (^{13}C) networks, although the relationship observed in the enriched community (^{13}C) network was weaker (^{12}C -network $R^2=0.66$ vs. ^{13}C -network $R^2=0.31$). The clearest pattern here is the strong, positive connection between predatory bacteria of the phylum Bdellovibrionota, such as *Peredibacter*, *Bacteriovorax*, and *Oligoflexus*, and various fungi.

Discussion

Ingrowth bags focus fungal-bacterial interactions

The ingrowth bags were effective in trapping soil fungi [42, 43], and although challenging, we were able to detect and identify ^{13}C enriched hyphosphere bacteria with this method. Different from plant-associated soil compartments (e.g., rhizosphere), in which microbes directly incorporate plant metabolites, the ingrowth bag system experiences a dilution of isotopic signals where ^{13}C from a pulse label is released by plant roots, consumed by rhizosphere fungi that extend beyond the rhizosphere into the ingrowth bags, and finally into the hyphosphere where they are assimilated by associated bacteria. This resulted in a system with low biomass and low overall ^{13}C -enrichment compared to the rhizosphere. Although the difference between the average DNA density in ^{12}C and ^{13}C samples was small (indicated by the small separation between DNA density curves in Supplemental

Fig. S3), the EAF values are within previously reported ranges in the hyphosphere [10, 11]. This shift in density was enough for us to detect the taxon-specific enrichment of ^{13}C signal in both fungi (39 OTUs) and bacteria (214 ASVs; Fig. 1). However, the number of bacteria that significantly incorporated ^{13}C (54 ASVs with lower confidence intervals greater than 0% ^{13}C EAF) was several times lower than previous studies on soil incubated with glucose [9], incorporated maize residues [44], and hyphosphere grassland soils [10, 11]. Notably, the majority of the highly ^{13}C -enriched bacterial genera that entered the ingrowth bags are motile (Fig. 2), consistent with the idea that they followed the “fungal highway” into the ingrowth bags. Since the bags were filled with nutrient-depleted quartz sand, the bacteria likely obtained nutrients through assimilation of hyphal exudates [12] or predate directly on the hyphae [13], leading to ^{13}C enrichment in their DNA. We cannot rule out the possibility that the bacteria could have also assimilated mobile nutrients that diffused passively into the bags, which is a limitation of the ingrowth bag method, but also reflects the difficulty of studying microbial interactions in the soil. Together, we found that although challenging, ingrowth bags are an environment that minimizes the complexity within the soil and thus are an advantageous system to study soil fungi, the bacteria that associate with them, as well as C dynamics in fungal-bacterial interactions in situ.

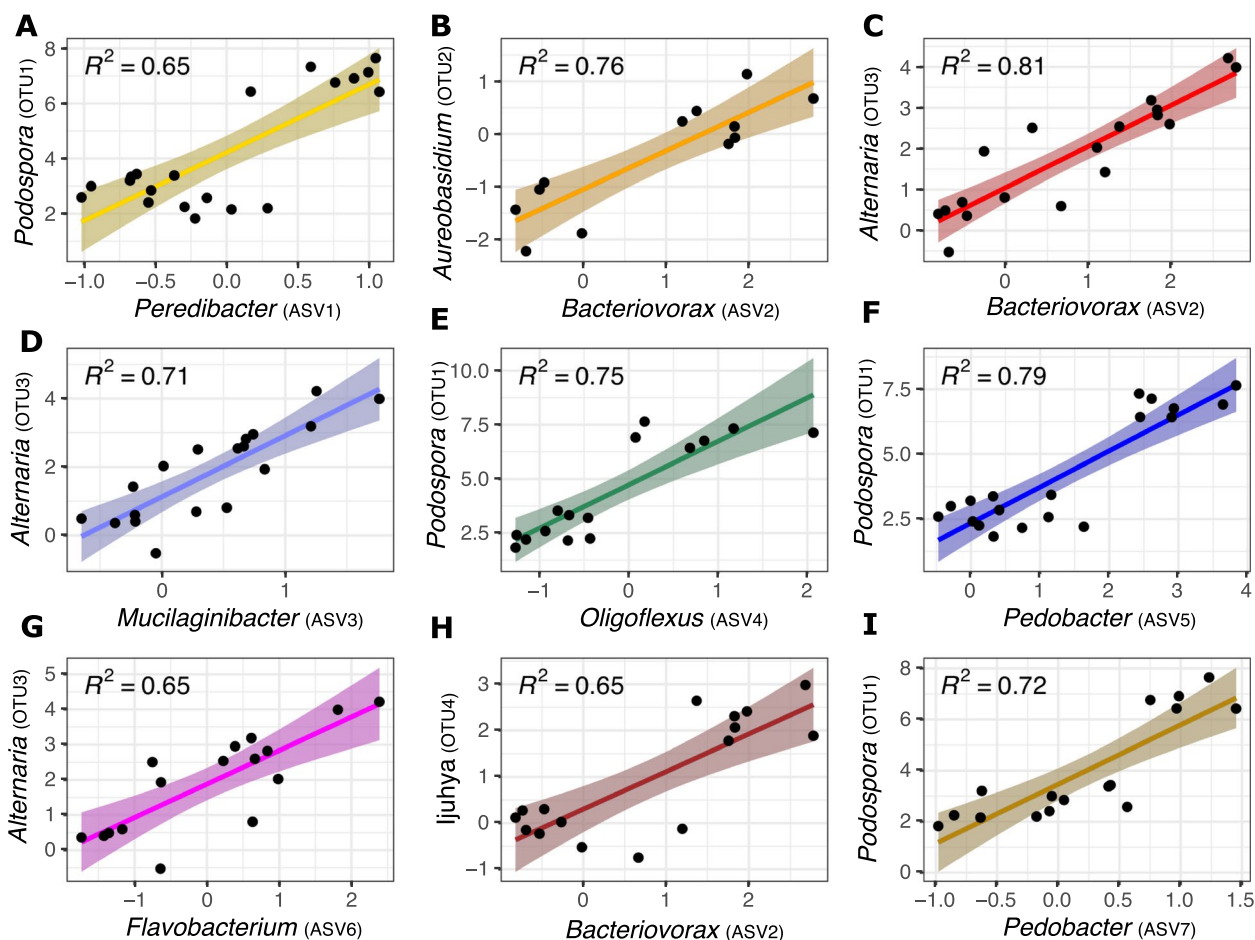


Fig. 4 Positive linear relationship among fungal and bacterial taxa that incorporated ^{13}C into their cells during a $^{13}\text{CO}_2$ plant labelling experiment in sand-filled ingrowth bags in a grassland soil identified through network analysis with $R^2 \geq 0.65$. Each dot represents the centered-log-ratio transformed abundance of the OTU/ASV found within a DNA fraction (see “Methods” section). While the fungi and bacteria presented were detected in all labeled samples, their relative abundance varied greatly across different ingrowth bags as well as fractions (Supplemental Fig. S4), resulting in clustering of the plotted values. Both axes are the centered-log-ratio transformed abundance of the specified fungi and bacteria. The colored area represents the relationship between fungi and bacteria predicted by the model. The R^2 value of the fitted model for each fungal-bacterial link is shown in each panel

Within the isolated ingrowth bag system, we found saprotrophic fungi to be highly ^{13}C -enriched. Saprotrophic fungi are pivotal decomposers in terrestrial ecosystems, catalyzing the conversion of complex organic compounds to more simple organic compounds, which are then available as either mycelium or hyphal exudates that can be consumed by bacteria. Indeed, it has been shown that fungal-bacterial interactions related to C acquisition occur by the utilization of fungal-released compounds by bacteria associated with hyphae [12] or through competitive interactions with the molecules liberated by fungi at the hyphal tips [45, 46]. Here, we found a small subset of fungi such as *Aspergillus* and *Coprinus*, that had significantly incorporated ^{13}C into their cells (Fig. 2). In contrast, we also found saprotrophic fungi that were

not enriched in ^{13}C . These were litter and wood saprotrophs of the genera *Mycoarthritis*, *Chaetomium*, *Bjerkandera*, *Xylodon*, among others. The ability of some fungi to assimilate ^{13}C suggests their ability, and perhaps preference, to consume root exudates rather than the more difficult to decompose plant polymers or stabilized soil organic matter. While this experiment cannot directly show the hyphosphere effect of litter or wood decomposing fungi, it is possible that they can effectively distribute and make available plant-derived C across soil compartments [47, 48].

As with saprotrophic fungi, we found biotrophic fungi, including plant pathogenic fungi like *Fusarium* and *Aureobasidium*, and animal parasite like *Ijuhya* highly ^{13}C -enriched (Fig. 2). Their direct connection to plant

roots (or animals that graze directly on plant roots) provides a direct pathway for ^{13}C to travel into the soil. It should be noted that these fungi can also have a saprotrophic lifestyle, therefore they may also distribute C through the saprotrophic pathway. Similarly, arbuscular mycorrhizal fungi (AMF) also have direct connections to plant C. While we found that 194 AMF OTUs did enter the ingrowth bags with low relative abundance (Supplemental Fig. S5), they were not detected as labeled taxa, perhaps due to their low GC DNA content [49, 50] that did not separate out well during the isotope fractionation. Therefore, we cannot rule out the fact that AMF, which are often highly labeled according to NanoSIMS measurements, can transfer a sizable pool of ^{13}C into the hyphosphere (Kakouridis et al. 2024), and that the ^{13}C enriched bacteria here may have also consumed ^{13}C from mycorrhizal fungi. While it has been a significant challenge to associate fungal-bacterial occurrence patterns to soil ecosystem functions [51], the patterns of saprotrophic and biotrophic fungi supporting associated bacteria reinforce the concept of bacterial nutrients exchange with fungi in adverse and nutrient-poor environments [52]. We propose that although these different fungal trophic guilds initially acquire plant C through different pathways, ultimately, they distribute and release plant-derived C beyond the rhizosphere through interactions with the hyphosphere microbiome.

We compared the results from this study with previous studies that used soils from an adjacent field site and found some insightful connections of fungi to the hyphosphere microbiome. Each of the study design allowed for an increased focus on the bacteria associated with hyphae. These ranged from soils with detritus [48], soils influenced by hyphae [11], soils with abundant and visible hyphae [10], and ingrowth bags that separated hyphae from surrounding soil (this study). While the phyla Actinobacteriota, Bacteriodota, Proteobacteria, and Verrucomicrobia (Fig. 1) are consistently represented across these studies, low representation of Acidobacteriota, Bacillodota, Chloroflexi, Plactomycetota, and ammonium oxidizing archaea in this study suggests that certain phyla are more connected to the complexity of the soil whereas others may be more dependent on the direct connection with fungal hyphae. For example, relative abundance, as well as ^{13}C enrichment of the bacteria phylum Proteobacteria changes in the presence of arbuscular-mycorrhizal fungi [11]. In particular, with the presence of hyphae, there is a higher abundance of predatory bacteria in the phyla Bdellovibrionota (this study) and Myxococcota (Nuccio et al. 2022). While the general biology of the Verrucomicrobia is largely unknown, their presence connected to

fungal hyphae suggests that at least some of the members of this group have some associations with fungi. These responses could be related to fungal-bacterial interactions in the hyphosphere. In contrast, we only detected a single ASV of the phylum Acidobacteria, which was commonly found in other studies and are often highly abundant in soils [53]. Their low enrichment here suggests that these common soil bacteria may not actively interact with labile fungal carbon. We observed an absence of labeled ammonium oxidizing archaea that was found in all other studies. Since saprotrophic and biotrophic fungi can make ammonium available through decomposition, we would expect a higher level of ammonium availability. However, within a quartz sand substrate that has low ammonium adsorption and availability [54, 55], low microbial biomass and therefore low CO_2 from respiration, there is little electron donor nor acceptors to support ammonium oxidizing archaea. These patterns of presence and absence gleaned through multiple studies of the same soil provided good insights into the occurrence between fungi and associated bacteria taxa, but additional approaches are required to build direct connections of their relationships and nature of interactions.

Isotope-enabled networks more precisely predict fungal-bacterial interactions

Understanding the mechanism of microbial interactions in soil has been a daunting challenge, and while isotopic in combination with 'omics methods allow us to detect trophic interactions where some form of nutrient exchange had occurred, they do not tell us which organisms might be interacting with each other. To make more concise predictions on specific microbes and their potential interactions, we built cross-domain networks with the organisms that have incorporated ^{13}C into their cells. This approach allowed us to narrow down and identify potentially interacting fungal-bacterial partners. We found that compared to the total community (^{12}C) network, the enriched community (^{13}C) network had a much higher complexity, with fewer nodes and more edges, and more fungal-bacterial links (Fig. 3). The majority of the highly ^{13}C -enriched fungi (6 of 9) that links to highly ^{13}C -enriched bacteria (46 of 54) in this nutrient-poor system suggests that the majority of the active bacteria were primarily associated with fungi in C exchange. This ^{13}C exchange was elegantly illustrated by [56], who showed that fungi can transfer nutrients to bacteria from nutrient-rich to nutrient-deprived habitats, highlighting the importance of fungal-bacteria interactions in nutrient-poor environments. While co-occurrence patterns based on

amplicon sequencing data are a useful tool to create hypothesis for further testing cross-domain interactions [57], the information regarding a specific nutrient dynamic might not be fully captured. Even though the higher number of fungal-bacterial interactions we observed in the enriched community (^{13}C) network may be an attribute of the lower RMT cut-off or the reduced number of features used to construct the network (as shown by the comparison with the mock network), enriched community (^{13}C) networks allowed us to detect more precise fungal-bacterial associations by narrowing down only taxa that have actively incorporated a labeled substrate. In complex environments such as the soil, the combination of isotopic and network analysis methods brings us a step closer to understanding the mechanisms of fungal-bacterial interactions in the context of nutrient dynamics.

The type of network links (positive or negative) allows us to infer the mode of interactions, such as the relationship among certain fungi and bacteria that are highly ^{13}C -enriched (Fig. 4). While the strong positive co-occurrence between *Alternaria* with *Mucilaginobacter* or *Flavobacterium*, and *Podospora* with *Pedobacter*, *Peredibacter*, or *Oligoflexus* suggest that both fungi and bacteria either increase or decrease in abundance, the mechanism of interactions is not clear. Notably, bacteria of the phylum Bdellovibrionota, such as *Peredibacter*, *Bacteriovorax*, and *Oligoflexus*, are prey-selective predatory bacteria, preying on gram-negative bacteria, are capable of incorporating ^{13}C labeled prey biomass [58], and are highly ^{13}C -enriched in this study. This amplification of isotopic signals occur in higher rates in predators, allowing them to achieve higher levels of substrate incorporation in a short period of time [10, 15]. These predatory taxa had strong positive co-occurrence with fungi but negative co-occurrence with certain gram-negative bacteria including *Perluclidibaca* and *Mucilaginibacter* (Supplemental Fig. S6). We would therefore expect that as the abundance of fungi increases, the abundance of bacteria that feed on fungal carbon also increases, followed by an increase in the abundance of predatory bacteria. Indeed, we found these patterns in this study. There was an increase in abundance of fungi (*Alternaria* and *Podospora*) with an increase in the abundance of bacteria (*Flavobacterium*, *Mucilaginobacter*, and *Pedobacter*) that consumed fungal carbon; an increase in abundance of predatory bacteria (*Peredibacter*, *Bacteriovorax*, and *Oligoflexus*); and a decrease in the abundance of certain gram-negative bacterial taxa (*Perluclidibaca* and *Mucilaginibacter*) as the abundance of predatory bacteria (*Bacteriovorax* and *Peredibacter*) increases. While these patterns require longitudinal experiments to confirm, the links

of the enriched community (^{13}C) network narrowed the complexity of soil fungal-bacterial interactions and provided an intriguing set of hypotheses to test inter-domain food webs in soil.

Study limitations and future considerations

The use of ingrowth bags, qSIP, and isotope-enabled networks gave us a powerful set of tools to narrow in on fungal-bacterial interactions in the hyphosphere, but we recognize that there are limitations that should be considered for future studies. We acknowledge that the small number of replications is a limitation of our study and therefore not representative across larger environments. Since more replicates and DNA density fractions are needed in order to identify taxon-specific enrichment in samples with lower isotopic enrichment [59], we combined fractions within similar density gradients into new binned fraction groups to yield enough DNA to sequence the maximum possible fractions (7 total) in our system. For studies considering using the same ingrowth bag system, we suggest deploying larger volume bags to increase biomass recovery, adding more replicates to potentially increase the number of significantly labeled taxa detected, and incorporating other 'omics techniques to better understand the functional contributions of the partners involved. We focused this study on fungal-bacterial interactions, therefore we did not discuss the bacterial-bacterial or fungal-fungal interactions, except for the case of predatory bacteria. Similarly, we did not study the many others organism that are part of the soil food web that are important drivers of soil C dynamics. As with any correlation methods, the inferences of ^{13}C fungal-bacterial interactions drawn from qSIP and co-occurrence network data should be synthesized critically, taking into consideration both ecological factors such as previously knowledge of the food-web (e.g., predatory bacteria), as well as methodological constrains (e.g., prevalence filtering methods and fractions within replicates not being not fully independent observations) associated with the study design. Nevertheless, the combination of the two methods allows us to detect the bacteria that have consumed presumably fungal ^{13}C and hypothesize their direct interactions that may be tested in future experiments.

This study demonstrated the utility of ingrowth bags, SIP, combined with analytical qSIP and co-occurrence network analysis to predict potential fungal-bacterial interactions in dynamic natural systems processes such as C cycling. Given that qSIP can quantify active taxa involved in a specific nutrient cycling process and co-occurrence networks have the ability to correlate their abundance patterns, in combination they provide means to identify potential trophic interactions such as predation and facilitative links as demonstrated in this study.

While there are drawbacks with these methods, they enabled us to focus on potential interactions that can be experimentally tested to further elucidate the mechanisms that underlie C dynamics. Ultimately, this novel approach provides significant progress towards building a mechanistic understanding of the complex nature of fungal-bacterial interactions in soil.

Supplementary Information

The online version contains supplementary material available at <https://doi.org/10.1186/s40168-025-02100-2>.

Additional file 1. Supplemental Figure S1. Venn diagram representing the number of taxa shared between the six physical sandbag samples (before fractionation for qSIP analysis) and six bulk soil samples collected from the corresponding plots. Amplicon sequencing targeting both bacteria (16S rRNA gene) and fungi (ITS gene) was performed using the same methods used to sequence the qSIP dataset. Supplemental Figure S2. Distribution of the number of ASV/OTUs that were kept after filtering for taxa that are present in at least 50% of samples to construct the (A) total microbial community network and (B) the enriched community network that is a result of a ^{13}C plant labelling experiment in sand-filled ingrowth bags. A total of 58 taxa were kept for the construction of the enriched community (^{13}C) network and 454 taxa were kept for the construction of the total community (^{12}C) network. The different colors represent the fractions of each sample and each bar represents a labeled or unlabeled sample. Supplemental Figure S3. Relative density shift of ^{12}C and ^{13}C DNA stable isotope probing density fractions extracted and density fractionated from sand-filled ingrowth bags after a ^{13}C plant labelling experiment in a grassland soil. For each single physical sample 1 μg of DNA was subjected to ultracentrifugation in a cesium chloride density gradient, then separated into fractions. Based on qPCR data, the proportion of total fungal (A) and bacterial/archaeal (B) gene copies as a function of DNA density from samples exposed to ^{13}C (red) or ^{12}C (blue). Dashed lines represent the average density of the DNA from ^{12}C and ^{13}C sample fractions. Supplemental Figure S4. Relative abundance of bacterial ASVs (A) and fungal OTUs (B) shown in Fig. 4. Relative abundance results were calculated based on the number of sequences reads for each ASV/OTU and total reads per fraction sample of sand-filled ingrowth bags after a ^{13}C plant labelling experiment in a grassland soil. The relative abundance of the bacterial ASVs and fungal OTUs varied greatly across different ingrowth bags as well as fractions. Supplemental Figure S5. Relative abundance of amplicon sequencing (ITS) data from the six physical sandbag samples investigated in this study before fractionation for qSIP analysis showing dominance of the phyla Ascomycota and Basidiomycota. Sequencing was performed using the same methods used to sequence the qSIP dataset. Fungal OTUs were grouped and colored by phyla. The relative abundance of each phylum was calculated based on the number of reads per phylum in each sample and the total number of reads per sample. Supplemental Figure S6. Negative linear relationship between predatory bacteria *Bacteriovorax* and gram-negative bacteria *Perilucidibaca* (A) and predatory bacteria *Peredibacter* and gram-negative bacteria *Mucilaginibacter* (B). Each dot represents the centered-log-ratio transformed abundance of the ASV found within a DNA fraction (see methods). Both axes represent the centered-log-ratio transformed abundance of the specified bacteria. The colored area represents the relationship between pairs predicted by the model. R^2 value of the fitted model is shown in each panel.

Additional file 2. Supplementary Table S1. List of all ^{13}C labeled taxa, average excess atom fraction (EAF) values, and 90% confidence intervals. Supplementary Table S2. Motility assignment and trophic guild information of all ^{13}C labeled bacteria and fungi respectively. Supplementary Table S3. Topological properties of the enriched community (^{13}C), total community (^{12}C), and mock networks. Supplementary Table S4. Total and fungal-bacterial links identified in the enriched (^{13}C) and the total (^{12}C) community networks.

Acknowledgements

We thank Karen Parada for assisting with DNA extractions, Daliang Ning for contributing valuable information related to cross-domain network calculations, Mike Allen for SIP processing, Bram Stone for providing helpful insights related to the qSIP calculation, Alexa Burger for assisting with qPCR analysis, and the Cross Kingdom Interactions sampling team for help with field set-up and sampling.

Authors' contributions

G.S. wrote the original draft. N.N. and G.S. conceptualization. N.N., M.Y., and K.E. performed experimental design and sample collection. S.B., M.A., A.C., and G.S. conducted sample processing. G.S. performed the analysis. N.N., M.F., and J.P. performed project supervision and acquired funding. All authors reviewed the manuscript.

Funding

This research was supported by the U.S. Department of Energy Office of Science, Office of Biological and Environmental Research Genomic Science program under Awards DE-SC0020163 and DE-SC0016247 to M.K.F. at UC Berkeley, Awards SCW1589 and SCW1678 to J.P.-R. at Lawrence Livermore National Laboratory, and Award DE-SC0023106 at the University of Hawai'i, Mānoa. Work conducted at Lawrence Livermore National Laboratory was supported under the auspices of the U.S. DOE under Contract DE-AC52-07NA27344. U.S. Department of Energy Office of Science, Office of Biological and Environmental Research Genomic Science program, DE-SC0020163 and DE-SC0016247, SCW1589 and SCW1678, DE-SC0023106, U.S. DOE, DE-AC52-07NA27344

Data availability

The dataset supporting the conclusions of this article is available in the Sequence Read Archive repository under accession PRJNA1120058. R commands for analyses are available at <https://github.com/nnguyenlab/sandbag-BFI>.

Declarations

Ethics approval and consent to participate

Non-applicable.

Consent for publication

Non-applicable.

Competing interests

The authors declare no competing interests.

Received: 23 November 2024 Accepted: 26 March 2025

Published online: 30 April 2025

References

- Fierer N. Embracing the unknown: disentangling the complexities of the soil microbiome. *Nat Rev Microbiol.* 2017;15(10):579–90.
- Hestrin R, et al. Plant-associated fungi support bacterial resilience following water limitation. *ISME J.* 2022;16(12):2752–62.
- Wang L, George TS, Feng G. Concepts and consequences of the hyphosphere core microbiome for arbuscular mycorrhizal fungal fitness and function. *New Phytol.* 2024;242(4):1529–33.
- Nguyen NH. Fungal hyphosphere microbiomes are distinct from surrounding substrates and show consistent association patterns. *Microbiol Spectr.* 2023;11(2): e0470822.
- Sokol NW, et al. Life and death in the soil microbiome: how ecological processes influence biogeochemistry. *Nat Rev Microbiol.* 2022;20(7):415–30.
- Wu H, et al. Unveiling the crucial role of soil microorganisms in carbon cycling: A review. *Sci Total Environ.* 2024;909: 168627.
- Wang C, Kuzyakov Y. Mechanisms and implications of bacterial-fungal competition for soil resources. *ISME J.* 2024;18(1):wrae073.

8. Deveau A, et al. Bacterial–fungal interactions: ecology, mechanisms and challenges. *FEMS Microbiol Rev.* 2018;42(3):335–52.
9. Hungate BA, et al. Quantitative microbial ecology through stable isotope probing. *Appl Environ Microbiol.* 2015;81(21):7570–81.
10. Nuccio EE, et al. HT-SIP: a semi-automated stable isotope probing pipeline identifies cross-kingdom interactions in the hyphosphere of arbuscular mycorrhizal fungi. *Microbiome.* 2022;10(1):199.
11. Kakouridis A, et al. Arbuscular mycorrhiza convey significant plant carbon to a diverse hyphosphere microbial food web and mineral-associated organic matter. *New Phytologist.* 2024. n/a(n/a).
12. Haq IU, et al. The interactions of bacteria with fungi in soil: emerging concepts. *Adv Appl Microbiol.* 2014;89:185–215. <https://doi.org/10.1016/B978-0-12-800259-9.00005-6>. PMID: 25131403.
13. Leveau JHJ, Preston GM. Bacterial mycophagy: definition and diagnosis of a unique bacterial–fungal interaction. *New Phytol.* 2008;177(4):859–76.
14. Fossium C, et al. Belowground allocation and dynamics of recently fixed plant carbon in a California annual grassland. *Soil Biol Biochem.* 2022;165: 108519.
15. Hungate A, et al. The functional significance of bacterial predators. *Mbio.* 2021;12(2):10–128. <https://doi.org/10.1128/mbio.00466-21>.
16. Yuan MM, et al. Fungal-bacterial cooccurrence patterns differ between arbuscular mycorrhizal fungi and nonmycorrhizal fungi across soil niches. *MBio.* 2021;12(2):10–128.
17. Heisey S, et al. A single application of compost can leave lasting impacts on soil microbial community structure and alter cross-domain interaction networks. *Front Soil Sci.* 2022;2:749212.
18. Liao H, et al. Complexity of bacterial and fungal network increases with soil aggregate size in an agricultural Inceptisol. *Appl Soil Ecol.* 2020;154: 103640.
19. Maillard F, et al. Melanization slows the rapid movement of fungal necromass carbon and nitrogen into both bacterial and fungal decomposer communities and soils. *mSystems.* 2023;8(4):e00390-23.
20. Sokol NW, et al. Divergent microbial traits influence the transformation of living versus dead root inputs to soil carbon. *bioRxiv.* 2022:2022.09.02.506384.
21. Parada AE, Needham DM, Fuhrman JA. Every base matters: assessing small subunit rRNA primers for marine microbiomes with mock communities, time series and global field samples. *Environ Microbiol.* 2016;18(5):1403–14.
22. Apprill A, et al. Minor revision to V4 region SSU rRNA 806R gene primer greatly increases detection of SAR11 bacterioplankton. *Aquat Microb Ecol.* 2015;75(2):129–37.
23. Taylor DL, et al. Accurate estimation of fungal diversity and abundance through improved lineage-specific primers optimized for Illumina amplicon sequencing. *Appl Environ Microbiol.* 2016;82(24):7217–26.
24. Nguyen NH, et al. Parsing ecological signal from noise in next generation amplicon sequencing. *New Phytol.* 2015;205(4):1389–93.
25. Bolyen E, et al. Reproducible, interactive, scalable and extensible microbiome data science using QIIME 2. *Nat Biotechnol.* 2019;37(8):852–7.
26. Callahan BJ, et al. DADA2: High-resolution sample inference from Illumina amplicon data. *Nat Methods.* 2016;13(7):581–3.
27. Rognes T, et al. VSEARCH: a versatile open source tool for metagenomics. *PeerJ.* 2016;4: e2584.
28. Quast C, et al. The SILVA ribosomal RNA gene database project: improved data processing and web-based tools. *Nucleic Acids Res.* 2012;41(D1):D590–6.
29. UNITE Community. UNITE QIIME release. Version 2021.05.10. 2021.
30. Nguyen NH, et al. FUNGuild: An open annotation tool for parsing fungal community datasets by ecological guild. *Fungal Ecol.* 2016;20:241–8.
31. Blazewicz SJ, et al. Taxon-specific microbial growth and mortality patterns reveal distinct temporal population responses to rewetting in a California grassland soil. *ISME J.* 2020;14(6):1520–32.
32. Op De Beeck M, et al. Comparison and validation of some ITS primer pairs useful for fungal metabarcoding studies. *PLOS ONE.* 2014;9(6): e97629.
33. Koch BJ, et al. Estimating taxon-specific population dynamics in diverse microbial communities. *Ecosphere.* 2018;9(1): e02090.
34. Kimbrel J. qSIP2: qSIP analysis. 2023. <https://github.com/jeffkimbrel/qSIP2>.
35. Orsi WD, et al. Carbon assimilating fungi from surface ocean to subseafloor revealed by coupled phylogenetic and stable isotope analysis. *ISME J.* 2022;16(5):1245–61.
36. Deng Y, et al. Molecular ecological network analyses. *BMC Bioinformatics.* 2012;13(1):113.
37. Tipton L, et al. Fungi stabilize connectivity in the lung and skin microbial ecosystems. *Microbiome.* 2018;6(1):12.
38. Quinn TP, et al. A field guide for the compositional analysis of any-omics data. *Gigascience.* 2019;8(9):giz107.
39. Lahti LS. Tools for microbiome analysis in R Version URL:<http://microbiome.github.com/microbiome>. 2017.
40. Bastian HS, Jacomy M. Gephi: an open source software for exploring and manipulating networks. In: *International AAAI Conference on Weblogs and Social Media.* 2009.
41. Aphalo PJ. *Learn R ...as you learnt your mother tongue.* Helsinki: Leanpub; 2016.
42. Johnson D, Leake JR, Read DJ. Novel in-growth core system enables functional studies of grassland mycorrhizal mycelial networks. *New Phytol.* 2001;152(3):555–62.
43. Branco S, Bruns TD, Singleton I. Fungi at a small scale: spatial zonation of fungal assemblages around single trees. *PLoS ONE.* 2013;8(10): e78295.
44. Dong W, et al. Linking microbial taxa and the effect of mineral nitrogen forms on residue decomposition at the early stage in arable soil by DNA-qSIP. *Geoderma.* 2021;400: 115127.
45. De Boer W, Van der Wal A. Interactions between saprotrophic basidiomycetes and bacteria. In Boddy L, Frankland JC, van West P, editors, *British Mycological Society Symposia Series, Volume 28.* Amsterdam: Elsevier B.V. 2008. p. 141–151.
46. Johnston SR, Boddy L, Weightman AJ. Bacteria in decomposing wood and their interactions with wood-decay fungi. *FEMS Microbiol Ecol.* 2016;92(11):fiw179.
47. Pausch J, et al. Small but active – pool size does not matter for carbon incorporation in below-ground food webs. *Funct Ecol.* 2016;30(3):479–89.
48. Nuccio EE, et al. Community RNA-Seq: multi-kingdom responses to living versus decaying roots in soil. *ISME Communications.* 2021;1(1):72.
49. Kobayashi Y, et al. The genome of *Rhizophagus clarus* HR1 reveals a common genetic basis for auxotrophy among arbuscular mycorrhizal fungi. *BMC Genomics.* 2018;19(1):465.
50. Tisserant E, et al. Genome of an arbuscular mycorrhizal fungus provides insight into the oldest plant symbiosis. *Proc Natl Acad Sci.* 2013;110(50):20117–22.
51. de Menezes AB, Richardson AE, Thrall PH. Linking fungal–bacterial co-occurrences to soil ecosystem function. *Curr Opin Microbiol.* 2017;37:135–41.
52. Steffan BN, Venkatesh N, Keller NP. Let's get physical: bacterial-fungal interactions and their consequences in agriculture and health. *J Fungi (Basel).* 2020;6(4).
53. Janssen PH. Identifying the dominant soil bacterial taxa in libraries of 16S rRNA and 16S rRNA genes. *Appl Environ Microbiol.* 2006;72(3):1719–28.
54. Wolkoff ML. Adsorption of ammonium sulfate by soils and quartz sand: preliminary communication. *Soil Sci.* 1917;3(6):561–4.
55. He Q, et al. Absorption of ammonium by three substrates materials in constructed wetland system. *Huan Jing Ke Xue.* 2024;45(3):1577–85.
56. Khan N, et al. Mycelial nutrient transfer promotes bacterial co-metabolic organochlorine pesticide degradation in nutrient-deprived environments. *ISME J.* 2023;17(4):570–8.
57. Goberna M, Verdú M. Cautionary notes on the use of co-occurrence networks in soil ecology. *Soil Biol Biochem.* 2022;166: 108534.
58. Zhang L, et al. Active predation, phylogenetic diversity, and global prevalence of myxobacteria in wastewater treatment plants. *ISME J.* 2023;17(5):671–81.
59. Sieradzki Ella T, et al. Measurement error and resolution in quantitative stable isotope probing: implications for experimental design. *mSystems.* 2020;5(4). <https://doi.org/10.1128/mSystems.00151-20>.

Publisher's Note

Springer Nature remains neutral with regard to jurisdictional claims in published maps and institutional affiliations.